Check for updates

Targeted design of porous materials without strong, directional interactions†

Megan O'Shaughnessy,[a] Peter R. Spackman, [iD][bcd] Marc A. Little, [iD][a]
Luca Catalano, [iD][a] Alex James, [iD][a] Graeme M. Day [iD] *[b] and Andrew I. Cooper [iD] *[a]

A porous molecular crystal (TSCl) was found to crystallise from dichloromethane and water during the synthesis of tetrakis(4-sulfophenylmethane). Crystal structure prediction (CSP) rationalises the driving force behind the formation of this porous TSCl phase and the intermolecular interactions that direct its formation. Gas sorption analysis showed that TSCl is permanently porous with selective adsorption of CO_2 over N_2, H_2 and CH_4 and a maximum CO_2 uptake of 74 cm^3 g^{-1} at 195 K. Calculations revealed that TSCl assembles *via* a combination of weak hydrogen bonds and strong dispersion interactions. This illustrates that CSP can underpin approaches to crystal engineering that do not involve more intuitive directional interactions, such as hydrogen bonding.

Materials with permanent porosity have widespread applications in areas such as gas storage,[1] separation,[2] and catalysis.[3] Over the past two decades, metal–organic frameworks (MOFs)[4] and covalent organic frameworks (COFs)[5,6] have emerged as promising classes of porous materials. The strong, directional bonding in MOFs and COFs stabilises the permanent porosity in these materials.[7]

Porous molecular crystals, by contrast, are solids where the molecular subunits interact *via* comparatively weak intermolecular interactions.[8] These crystals can have either intrinsic or extrinsic porosity. Intrinsic porosity refers to porosity within the molecular subunits, as found in macrocycles[9] and porous organic cages (POCs).[10] Extrinsic porosity occurs when rigid molecular subunits pack inefficiently, creating pores between the molecules; examples of extrinsically porous molecular materials are hydrogen bonded organic frameworks (HOFs).[11] To have true extrinsic porosity, the material must maintain its voids after removal of the guest solvent molecules from the pores.[12] This is a challenge for porous molecular crystals, where close packing is typically energetically favoured. Extrinsic permanent porosity results from the interplay between the rigidity and geometrical shape of the molecular building blocks and the strength and directionality of their intermolecular interactions. This is exemplified by Dianin's compound (4-*p*-hydroxyphenyl-2,2,4-trimethylchroman), which forms inclusion compounds with a range of guest molecules and whose host framework is retained in the absence of guests;[13,14] hydroxyl groups form hydrogen-bonded rings which, combined with Dianin's compound's awkward molecular shape, prevent close-packing, leading to the formation of 1-dimensional channels in the host crystal structure. Other classic examples include the porous van der Waals crystals reported by Sozzani and coworkers.[15,16]

Over the last decade, HOFs have come to be one of the most widely studied classes of porous molecular crystals.[17] The most commonly used functional groups in HOFs are 2,4-diaminotriazinyl (DAT) and carboxylic acids due to the strength and directionality of the resulting hydrogen bonds.[18] In the quest to design and synthesise novel molecular porous crystals, we turned our attention to a tetrahedral tetraphenylmethane[19,20] derivative functionalised with sulfonyl groups (SO_2Cl), which have been reported to form cooperative S–Cl···O halogen bonding in α,ω-di(sulfonyl chloride) perfluoroalkanes.[21] Out aim was to find alternative non-covalent self-assembly motifs for porous molecular crystals.

We report the first example of a porous molecular crystal, **TSCl**, that uses a sulfonyl chloride as the directing functional group. To do this, the tetrahedral tecton, tetraphenylmethane, was functionalised with sulfonyl chloride groups. CSP has previously been shown to be able to predict the structures of inclusion compounds:[22] here by using CSP, we could predict

[a] *Materials Innovation Factory and Department of Chemistry, University of Liverpool, Liverpool, L7 3NY, UK. E-mail: aicooper@liverpool.ac.uk*

[b] *Computational System Chemistry, School of Chemistry, University of Southampton, Southampton, SO17 1BJ, UK. E-mail: G.M.Day@soton.ac.uk*

[c] *Leverhulme Research Centre for Functional Materials Design, Department of Chemistry and Materials Innovation Factory, University of Liverpool, Liverpool, L7 3NY, UK*

[d] *Curtin Institute for Computation, School of Molecular and Life Sciences, Curtin University, PO Box U1987, Perth, Western Australia 6845, Australia*

the formation of the porous **TSCl** structure and, subsequently, use theoretical calculations to understand the molecular interactions in the crystal structure. **TSCl** crystallises into a network containing open channels directly during its synthesis, and it can be activated readily to exhibit permanent porosity.

TSCl was synthesised by slowly adding an excess of chlorosulfonic acid to tetraphenylmethane in anhydrous dichloromethane (DCM) under an inert atmosphere. The addition of the reaction mixture to ice led to the instant precipitation of **TSCl** in an 82% yield (see ESI,† Scheme S1). **TSCl** was isolated in high purity directly as a precipitate from the reaction, as confirmed by ^{1}H and ^{13}C NMR (see ESI,† Fig. S1).

Single crystals of **TSCl** that were suitable for single crystal X-ray diffraction (SCXRD) were isolated by slowly evaporating 1,1,1,3,3,3-hexafluoro-2-propanol (HIPF), affording single crystals within 3 days. SCXRD reveals that **TSCl** crystallises in the tetragonal space group $I4$ with $\frac{1}{4}$ of the molecule residing in the asymmetric unit. In the crystal structure, each molecule can be viewed as connected to four neighbouring molecules using intermolecular interactions creating a 3D architecture containing tubular channels along the c axis. Using CrystalExplorer model energies,[23,24] the intermolecular interactions in **TSCl** consist of weak hydrogen bonding from the sulfonic oxygens and strong dispersive interactions from the chlorine atoms. There are additional weak hydrogen bonding interactions from the oxygens and hydrogens on the benzene rings. A search of the Cambridge Structural Database (CSD) for the Ph–SO$_2$Cl···O motif in **TSCl** (see ESI,† Fig. S11) gave seven results; all of these structures were densely packed (see ESI,† Fig. S12 and S13). In the seven CSD hits, the most common intermolecular interaction appears to be the halogen bond between the chlorine and oxygen atoms.[25–27] For the interaction between the chlorine and oxygen to be classified as halogen bonding, the distances are typically less than the sum of the van der Waals radii,[28–30] which is 3.27 Å. To our surprise, in **TSCl** the distance between the Cl and O is 3.45 Å and 3.70 Å (Fig. 1b), suggesting that the chlorine atom is not involved in any typical halogen bonding interactions.

Preliminary rigid-molecule CSP was performed on an ensemble of 17 unique conformers from a gas-phase conformer search to assess the viability of prediction for this molecule. The method used a distributed multipole-based atom–atom force field[31] for intermolecular interactions and a quasi-random search for generation of trial crystal structures. Full details, including the generation of conformers and the CSP methodology are provided in the ESI.† The preliminary CSP results on the gas-phase conformer ensemble produced no good match for the experimental **TSCl** structure. As a test of whether the effect of the polar environment in the crystal on molecular conformations could be significant, CSP was subsequently performed on the ensemble of 17 unique conformers after optimization in a molecular crystal-like dielectric. Likewise, the distributed multipole analysis was performed on the optimised electron density with the dielectric model of the crystalline environment.[32]

A notable 'spike' in the energy *versus* density distribution of predicted crystal structures was found at a density of
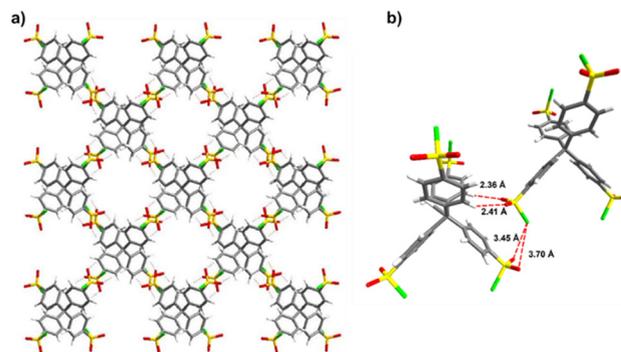
Fig. 1 (a) Packing of **TSCl** viewed down the c-axis showing the open accessible voids, (b) the intermolecular interactions in **TSCl**.

approximately 1.3 g cm^{-3} (Fig. 2a). Such low-density spikes have been found in several cases to correspond to observable porous crystal structures.[33,34] This porous crystalline structure (**TSCl-1**), roughly 10 kJ mol^{-1} higher in lattice energy than the predicted global minimum energy structure (see ESI,† Fig. S9), was found to reproduce the experimental **TSCl** crystal structure closely (Fig. 2b). It is worth noting that the molecular geometry in the experimental structure does not correspond to a minimum in the gas-phase—free optimization in the absence of the dielectric environment distorts the molecular geometry significantly—whereas the aforementioned crystal-like dielectric leads to a good match to the molecular conformation in the experimental crystal. This in turn leads to successful reproduction of the experimental crystal structure. Indeed, the set of molecular conformations in the gas-phase are quite distinct from those found when a crystal-like dielectric environment is introduced (see Table S2 in the ESI†). We conclude that the effect of the crystalline environment on molecular structure is important for this structure and, in this case, it is successfully modelled by introducing a continuum dielectric during generation of the conformational ensemble that was input into CSP. The polarizing environment also influences electrostatic interactions, resulting in the observed shift in calculated lattice energies (Fig. 2a) and making the low-density spike more prominent. However, this enhancement of electrostatic interactions seems to be less crucial in reproducing the observed porous crystal structure than the influence of the polarising environment on the molecular geometry.

Powder X-ray diffraction (PXRD) analysis showed that this porous **TSCl** phase was formed during the synthesis of tetrakis(4-sulfophenyl)methane and indicated that the crystalline material was phase pure (see ESI,† Fig. S4). Although the porous structure of **TSCl** was obtained directly from the reaction solvent, attempting to activate it proved difficult because of the large volume of strongly-bound water that was contained within the pores, which was approximately 13 wt%, as revealed by thermogravimetric analysis.

To allow for a simpler activation process that avoids high activation temperatures, **TSCl** was therefore first recrystallised. The solvents chosen for the recrystallisation were HIFP and

a)

b)
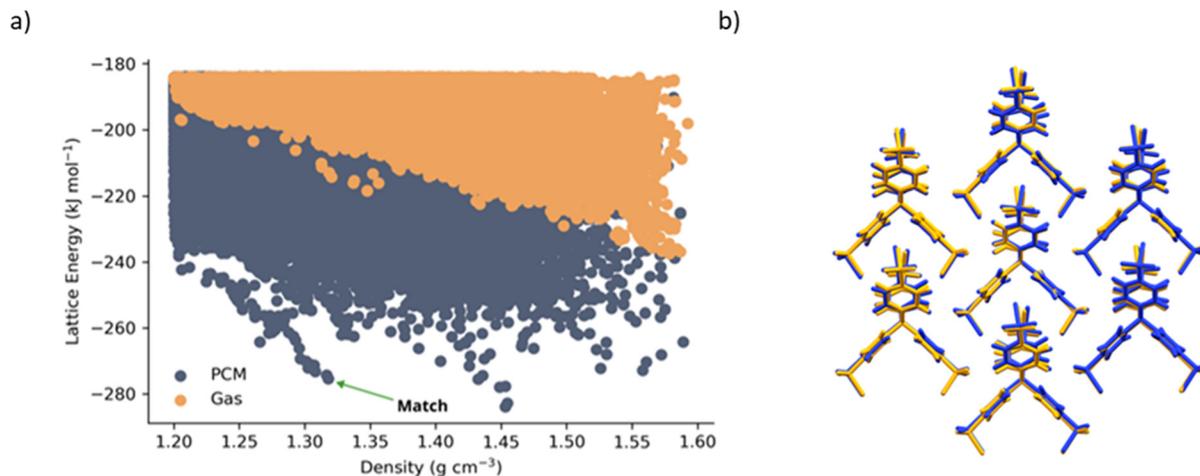
Fig. 2 (a) CSP energy-density landscape for **TSCl**. 'PCM' indicates conformers were optimised in a crystal-like dielectric (ε = 4) along with the subsequent distributed multipole analysis, whereas 'gas' indicates the usual isolated gas-phase molecular geometries and electron densities were used. (b) Structural overlay of the experimental (orange) and predicted (blue) structure of **TSCl**, rendered using Mercury[35]

methyl acetate (MeOAc). These solvents were selected because of their high vapour pressures at room temperature (20–25 °C), with HIFP having a vapour pressure of 16 kPa and MeOAc 28.8 kPa, compared to 2.4 kPa for water. The addition of MeOAc to HIPF resulted in **TSCl** instant precipitation with high crystallinity, thus allowing for a fast and simple recrystallisation process. Fig. S6 (ESI†) shows the difference in solvent retention before and after recrystallising **TSCl** from HIFP/MeOAc, where the weight percentage of solvent has decreased from 25% when isolated straight from the reaction to 7% after the recrystallization.

The recrystallised **TSCl** material was activated before gas sorption analysis by holding the sample under a nitrogen flow for several hours before being held under a dynamic vacuum at RT on the gas port. The gas sorption isotherms show that **TSCl** selectively adsorbs CO_2 over N_2, CH_4 and H_2 (Fig. 3). The low adsorption of H_2 (8 cm^3 g^{-1}) is likely due to the weak interaction of the molecules with the structure due to the small kinetic diameter (289 pm) of the H_2 molecules allowing the gas to move through the open channels freely. The quadrupole moment of CO_2 is approximately three times that of N_2,[36] which might allow the CO_2 molecules to form stronger electrostatic interactions with the sulfonate oxygens of the **TSCl** structure, providing a possible explanation for the CO_2/N_2 selectivity. It is also possible that diffusion of N_2 is kinetically restricted in this small-pore molecular crystal at 77 K; indeed, the hysteresis in the CO_2 isotherm at 195 K also suggests that equilibrium has not been reached, and this hysteresis decreases at higher temperatures. This lack of N_2 uptake in molecular crystals with small micropores at low temperatures is relatively common. The **TSCl** structure had a maximum CO_2 uptake of 74 cm^3 g^{-1} at 195K, which is comparable to or greater than other reported porous molecular crystals, including HOF-7a (28 cm^3 g^{-1}),[37] HOF-3a ($\sim$50 cm^3 g^{-1}),[38] and HOF-GS-10 ($\sim$42 cm^3 g^{-1}),[39] all of which also showed selective adsorption of CO_2 over N_2. PXRD was used to monitor the stability of **TSCl** to activation and
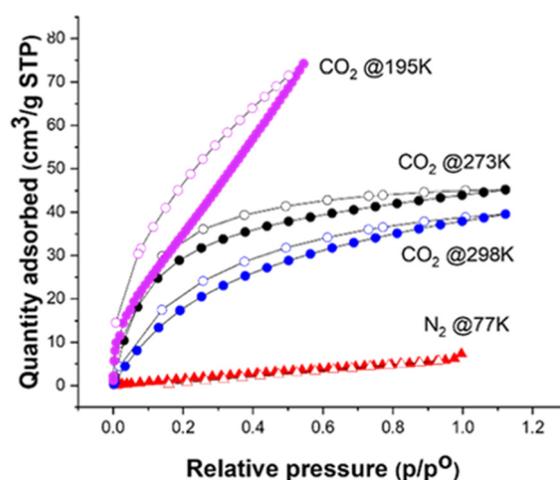
Fig. 3 Gas sorptions isotherms for **TSCl** show selectivity for CO_2 over N_2. Filled symbols are for adsorption, and the open symbols for desorption. See ESI,† Fig. S8 for H_2 and CH_4 isotherms.

sorption cycles and showed the TSCl remained unchanged (see ESI,† Fig. S9).

In summary, we have found a novel sulfonyl chloride porous molecular crystal, **TSCl**, which unlike most porous molecular crystals does not pack into a porous structure *via* strong directional interaction such as hydrogen bonds. Rather, the porous channels in **TSCl** are a result of the molecular shape of the tetrahedral molecular core, coupled with a combination of weaker intermolecular interactions. **TSCl** crystals can be grown rapidly from solution and recrystallised within minutes from volatile solvents, which allows for the material to be activated at room temperature under dynamic vacuum. The gas sorption results show that **TSCl** has permanent porosity, with the structure showing selectivity for CO_2 over N_2. The material adsorbs a relatively large amount of CO_2 compared to other materials in this class, such as HOFs.

We believe this work has implications for future design of porous materials, where the molecular shape of the molecule and the peripheral functional groups are used for the materials design, rather than relying so much on strong directional interactions, such as carboxylic acid dimers, or benzimidazalone groups.[40] The use of CSP unlocks this design approach: for example, we do not expect all tetraphenylmethane derivatives to generate porous structures, but chemical knowledge and intuition can fail us in terms of choosing which functionalities to use. CSP methods offer a straightforward way to make this choice – for example, by choosing functionalities that lead to low-energy 'spikes' of stable porous structures such as shown in Fig. 2a, or energy landscapes where the global energy minimum is porous, as is the case for Dianin's compound.[22] The use of highly directional supramolecular tectons has been successful, but these intuitive design rules are not infallible, and it does limit us to a restricted palette of functionalities, such as carboxylic acids. CSP methods unlock a straightforward method to broaden the range of chemistries that we can consider in supramolecular chemistry. Moreover, the timescales for these CSP calculations using modern methods and hardware are now competitive with the timescale for experimental synthesis and characterization: for example, the data shown in Fig. 2a required approximately 50 thousand CPU hours and could be obtained in around 48 hours on a shared high-performance computing system.

Conflicts of interest

There are no conflicts to declare.

Notes and references

1 S. S. Han, H. Furukawa, O. M. Yaghi and W. A. Goddard, *J. Am. Chem. Soc.*, 2008, **130**, 11580–11581.
2 P. Li, Y. He, H. D. Arman, R. Krishna, H. Wang, L. Weng and B. Chen, *Chem. Commun.*, 2014, **50**, 13081–13084.
3 Y. Zhang, X. Yang and H.-C. Zhou, *Polyhedron*, 2018, **154**, 189–201.
4 H. Li, M. Eddaoudi, M. O'Keeffe and O. M. Yaghi, *Nature*, 1999, **402**, 276–279.
5 F. J. Uribe-Romo, C. J. Doonan, H. Furukawa, K. Oisaki and O. M. Yaghi, *J. Am. Chem. Soc.*, 2011, **133**, 11478–11481.
6 X. Wang, L. Chen, S. Y. Chong, M. A. Little, Y. Wu, W.-H. Zhu, R. Clowes, Y. Yan, M. A. Zwijnenburg, R. S. Sprick and A. I. Cooper, *Nat. Chem.*, 2018, **10**, 1180–1189.
7 O. M. Yaghi, *J. Am. Chem. Soc.*, 2016, **138**, 15507–15509.
8 A. G. Slater and A. I. Cooper, *Science*, 2015, **348**, 6238.
9 S. Dawn, M. B. Dewal, D. Sobransingh, M. C. Paderes, A. C. Wibowo, M. D. Smith, J. A. Krause, P. J. Pellechia and L. S. Shimizu, *J. Am. Chem. Soc.*, 2011, **133**, 7025–7032.
10 T. Hasell and A. I. Cooper, *Nat. Rev. Mater.*, 2016, **1**, 16053.
11 J. Luo, J.-W. Wang, J.-H. Zhang, S. Lai and D.-C. Zhong, *CrystEngComm*, 2018, **20**, 5884–5898.
12 L. J. Barbour, *Chem. Commun.*, 2006, 1163–1168.
13 J. L. Flippen, J. Karle and I. L. Karle, *J. Am. Chem. Soc.*, 1970, **92**, 3749–3755.
14 R. M. Barrer and V. H. Shanson, *J. Chem. Soc., Chem. Commun.*, 1976, 333–334.
15 P. Sozzani, A. Comotti, R. Simonutti, T. Meersmann, J. W. Logan and A. Pines, *Angew. Chem., Int. Ed.*, 2000, **39**, 2695–2699.
16 P. Sozzani, S. Bracco, A. Comotti, L. Ferretti and R. Simonutti, *Angew. Chem., Int. Ed.*, 2005, **44**, 1816–1820.
17 R.-B. Lin, Y. He, P. Li, H. Wang, W. Zhou and B. Chen, *Chem. Soc. Rev.*, 2019, **48**, 1362–1389.
18 J. A. Zerkowski, J. C. MacDonald and G. M. Whitesides, *Chem. Mater.*, 1994, **6**, 1250–1257.
19 I. Bassanetti, S. Bracco, A. Comotti, M. Negroni, C. Bezuidenhout, S. Canossa, P. P. Mazzeo, L. Marchió and P. Sozzani, *J. Mater. Chem. A*, 2018, **6**, 14231–14239.
20 G. Xing, I. Bassanetti, S. Bracco, M. Negroni, C. Bezuidenhout, T. Ben, P. Sozzani and A. Comotti, *Chem. Sci.*, 2019, **10**, 730–736.
21 X. Liu, C. D. McMillen and J. S. Thrasher, *New J. Chem.*, 2018, **42**, 10484–10488.
22 A. J. Cruz-Cabeza, G. M. Day and W. Jones, *Chem. – Eur. J.*, 2009, **15**, 13033–13040.
23 C. F. Mackenzie, P. R. Spackman, D. Jayatilaka and M. A. Spackman, *IUCrJ*, 2017, **4**, 575–587.
24 P. R. Spackman, M. J. Turner, J. J. McKinnon, S. K. Wolff, D. J. Grimwood, D. Jayatilaka and M. A. Spackman, *J. Appl. Crystallogr.*, 2021, **54**, 1006–1011.
25 H. Christoph, J. Grunenberg, H. Hopf, I. Dix, P. G. Jones, M. Scholtissek and G. Maier, *Chem. – Eur. J.*, 2008, **14**, 5604–5616.
26 S. D. Robertson, A. M. Z. Slawin and J. D. Woollins, *Acta Crystallogr., Sect. E*, 2006, **E62**, o744–o745.
27 M. Treskow, J. Neudörfl and R. Giernoth, *Eur. J. Org. Chem.*, 2009, 3693–3697.
28 A. Bondi, *J. Phys. Chem.*, 1964, **68**, 441–451.
29 L. Brammer, *Faraday Discuss.*, 2017, **203**, 485–507.
30 H. Eramian, Y.-H. Tian, Z. Fox, H. Z. Beneberu and M. Kertesz, *J. Phys. Chem. A*, 2013, **117**, 14184–14190.
31 S. L. Price, M. Leslie, G. W. A. Welch, M. Habgood, L. S. Price, P. G. Karamertzanis and G. M. Day, *Phys. Chem. Chem. Phys.*, 2010, **12**, 8478–8490.
32 T. G. Cooper, K. E. Hejczyk, W. Jones and G. M. Day, *J. Chem. Theory Comput.*, 2008, **4**, 1795–1805.
33 A. Pulido, L. J. Chen, T. Kaczorowski, D. Holden, M. A. Little, S. Y. Chong, B. J. Slater, D. P. McMahon, B. Bonillo, C. J. Stackhouse, A. Stephenson, C. M. Kane, R. Clowes, T. Hasell, A. I. Cooper and G. M. Day, *Nature*, 2017, **543**, 657–664.
34 P. Cui, D. P. McMahon, P. R. Spackman, B. M. Alston, M. A. Little, G. M. Day and A. I. Cooper, *Chem. Sci.*, 2019, **43**, 9988–9997.
35 C. F. Macrae, I. Sovago, S. J. Cottrell, P. T. A. Galek, P. McCabe, E. Pidcock, M. Platings, G. P. Shields, J. S. Stevens, M. Towler and P. A. Wood, *J. Appl. Crystallogr.*, 2020, **53**, 226–235.
36 C. Graham, J. Pierrus and R. E. Raab, *Mol. Phys.*, 1989, **4**, 939–955.
37 W. Yang, B. Li, H. Wang, O. Alduhaish, K. Alfooty, M. A. Zayed, P. Li, H. D. Arman and B. Chen, *Cryst. Growth Des.*, 2015, **15**, 2000–2004.
38 P. Li, Y. He, Y. Zhao, L. Weng, H. Wang, R. Krishna, H. Wu, W. Zhou, M. O'Keeffe, Y. Han and B. Chen, *Angew. Chem., Int. Ed.*, 2014, 574–577.
39 A. Karmakar, R. Illathvalappil, B. Anothumakkool, A. Sen, P. Samanta, A. V. Desai, S. Kurungot and S. K. Ghosh, *Angew. Chem., Int. Ed.*, 2016, **55**, 10667–10671.
40 M. Mastalerz and I. M. Oppel, *Angew. Chem., Int. Ed.*, 2012, **51**, 5252–5255.